Dislocation-induced deep electronic states in InP: Photocapacitance measurements

Yutaka Oyama,[1] Jun-ichi Nishizawa,[2] Toshihiro Kimura,[1] and Takenori Tanno[2]
[1]*Department of Materials Science and Engineering, Graduate School of Engineering, Tohoku University, Aramaki Aza Aoba 6-6-11-1020, Sendai 980-8579, Japan*
[2]*Semiconductor Research Institute of Semiconductor Research Foundation, Aramaki Aza Aoba 519-1176, Sendai 980-0845, Japan*
(Received 21 June 2006; revised manuscript received 13 October 2006; published 12 December 2006)

Photocapacitance and excitation photocapacitance methods were applied to reveal the dislocation-induced deep levels in coalescent epitaxial lateral overgrowth layers of InP. Point-contact Schottky barrier junctions with small junction areas were formed on dislocated and dislocation-free regions by using wedge wire-bonding of Au, and photocapacitance measurements were then carried out at 30 K. In the dislocation-free layers, the dominant deep level was located at 1.30 eV below the conduction band, whereas in the dislocated area, dominant deep levels were detected at 0.86 eV ($\lambda = 1.44$ μm) and 1.05 eV ($\lambda = 1.18$ μm) below the conduction band. A neutralized state was also detected at 0.66 eV above the valence band. From the detailed excitation photocapacitance results, it is shown that the defect configuration coordinate diagram of the dislocation-induced deep levels was considered with large Frank-Condon shifts (d_{FC}) of 0.28 eV. This means that the atomic configurations around the deep levels are highly relaxed, as expected from the structures of the dislocation cores.

DOI: 10.1103/PhysRevB.74.235210 PACS number(s): 71.55.Eq, 71.20.Nr

I. INTRODUCTION

Dislocation-related electronic states in semiconductors have been investigated for a long time, even since the 1950s, by means of experimental and theoretical methods[1] due to their importance in solid state physics and for potential applications in industry. Indeed, electroluminescence[2] and 1.5 μm-Si light-emitting diodes[3] based on dislocation-related states have already been proposed.

It has been reported that dislocations form deep levels and shallow levels in semiconductors[4] depending on the atomic-configurations of the dislocation-core dangling bonds, the reconstructions of the defect configurations, and the strains around the dislocations. However, it is sometimes not easy to show that the detected electronic states really originate from the dislocations themselves.

The usual method for investigating dislocation-related states is the introduction of dislocations by plastic deformation at high temperature, followed by deep-level transient spectroscopy (DLTS),[5–7] photoluminescence (PL),[8] and electron spin resonance (ESR),[9] etc., being applied. Misfit dislocation-related deep levels have also been reported for some semiconductor heterostructure systems.[10]

The effects of impurity segregation at the dislocation core are also under discussion.[11] This is the so-called Cottrell atmosphere,[12] in which impurities are segregated around the dislocation core in order to compensate lattice strain. In addition, PL emissions from point defect clusters at the dislocation core have been also reported.[13] Based on this effect, the intrinsic gettering technique[14] is used for the improvement of electronic device performance. From these phenomena, it is not easy to gain evidence for a one-to-one correspondence for dislocations with respect to the detected deep levels.

On the other hand, investigations of gap states have been performed on the nanometer scale by surface tunneling spectroscopy (STS).[15] STS is one of the most promising techniques because individual dislocation cores can be identified on an atomic scale. However, it should be noted that the structure of the surface is usually reconstructed, and thus the defect structure on the surface may be different from that of the bulk state.

In this paper, the dislocations are introduced by the coalescence of dislocation-free epitaxial lateral overgrowth (ELO) layers of InP. It is known that the ELO technique has been applied to silicon-on-insulator (SOI) structures,[16] and it has also been successfully applied to GaN-based blue lasers.[17] The structures of the dislocation networks in the coalescent regions have been investigated[18] by cross-sectional TEM and their effects on the luminescence properties have been reported.[19] It has also been reported that dislocation-free ELO layers can be grown epitaxially by using an L-shaped open seed region,[20] which is an analogy for the kink-step structure on the macroscale. Dislocations were introduced selectively only at the coalescent region of two dislocation-free ELO layers. Then, a small-area Schottky barrier (SB) junction was formed by Au wire bonding at the dislocations, after which photocapacitance measurements were performed to detect only the dislocation-induced deep levels. The dislocated and dislocation-free ELO layers were grown on the same substrate in the same epitaxial growth run, and thus run-to-run fluctuations in growth conditions can be safely ignored in the present experiments. The photocapacitance results between dislocation-free and dislocated ELO layers were then compared, and the defect configuration coordinate diagram is discussed based on the excitation photocapacitance results.

II. EXPERIMENT

ELO was performed on Si-doped n^+-InP substrates with the (001) orientation by liquid phase epitaxy (LPE) at constant growth temperature. Prior to LPE growth, SiN layers of 100–200 nm thickness were deposited on the substrates by

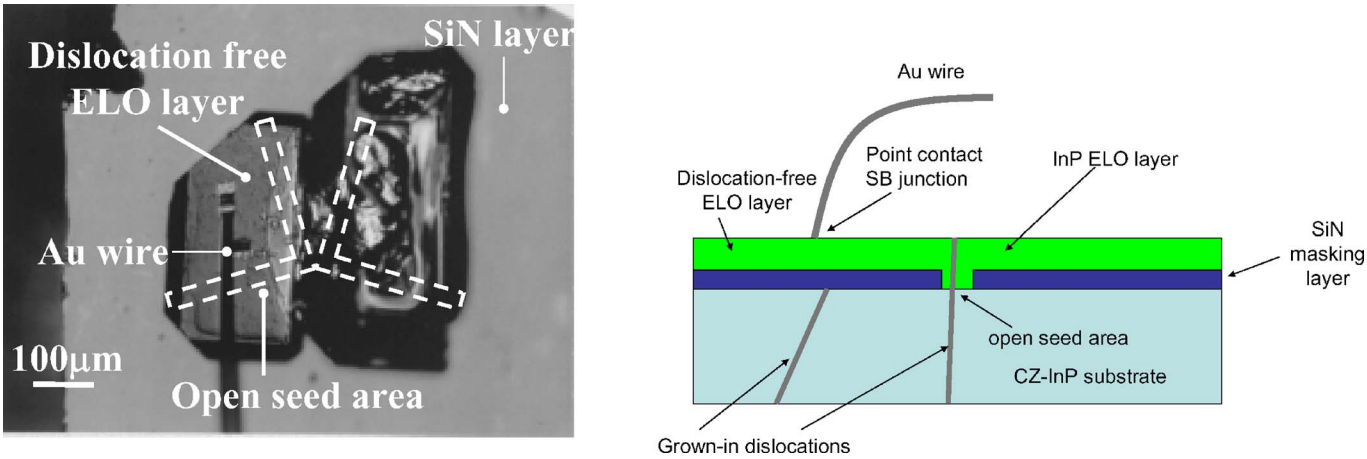

FIG. 1. (Color online) Microphotograph of a point-contact SB junction formed on a dislocation-free ELO layer and the corresponding schematic cross-sectional structure.

remote-plasma chemical vapor deposition (CVD) at 220 °C. L-shaped patterns of 30 μm width and 300–500 μm length were formed on the SiN/InP by using conventional photolithography and wet etching processes.

Prior to epitaxy, the substrates were degreased and lightly etched by about 50 nm using an H_2SO_4-based solution. LPE growth was carried out by the temperature difference method under controlled vapor pressure (TDM-CVP) in a Pd-diffused H_2 atmosphere. A temperature difference was induced in the solution, and thus the epitaxial growth proceeded at constant substrate temperature of 650 °C. The thickness of the epitaxial ELO layer was about 20 μm. A detailed description of LPE by TDM-CVP can be referred to elsewhere.[21] After epitaxial growth, the etch pit distribution on the ELO layers was determined by defect-etching using Huber etchant.[22]

After LPE growth, triangular-shaped ELO layers were formed from the "L"-shaped open seed region. It was shown that the surface of the ELO layers was atomically flat under the present growth conditions. The Huber etchant revealed no dislocations in the L-shaped ELO layers, implying that it is free of dislocations.

When two facing "L"-shaped open seed regions were used, square-shaped ELO layers were formed. It was shown that a high density of dislocations was introduced at the coalescent region between the two L-shaped ELO layers.

The dislocation-free L-shaped ELO layers and the dislocated coalescent ELO layers were grown epitaxially on same n^+-InP substrates in the same growth run. Thus, run-to-run fluctuations in growth conditions can be safely ignored.

The ELO layer exhibited n-type conductivity, with a carrier concentration of about 10^{16} cm^{-3} at RT. Therefore, the residual impurity concentration is reasonably low. Temperature-dependent Hall effect measurements were used to determine the activation energy of donor states, which was found to be about 5 meV. Secondary-ion-mass spectroscopy (SIMS) measurements also failed to reveal any traces of metal contamination in the layers.

In order to evaluate the deep levels, small-area SB junctions were formed on the dislocation-free and dislocated regions of the ELO layers by using the wedge wire bonding of Au, after which photocapacitance and excitation photocapacitance measurements were performed at 30 K. Details of the photocapacitance equipment and the measurement sys-

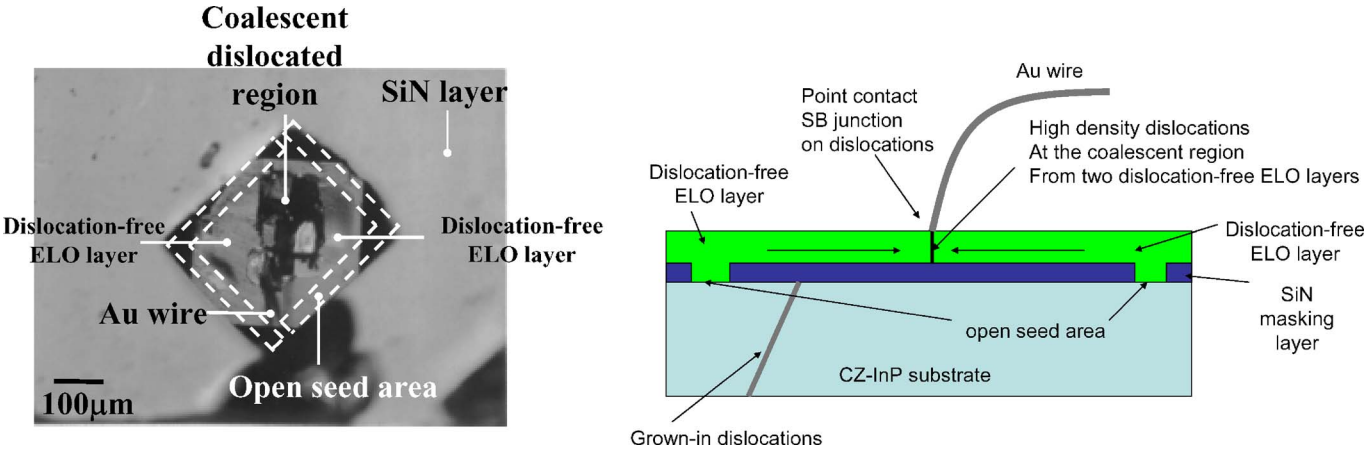

FIG. 2. (Color online) Microphotograph of a point-contact SB junction formed on a specific dislocated region, where the two dislocation-free ELO layers coalescence and the corresponding schematic cross-sectional structure.

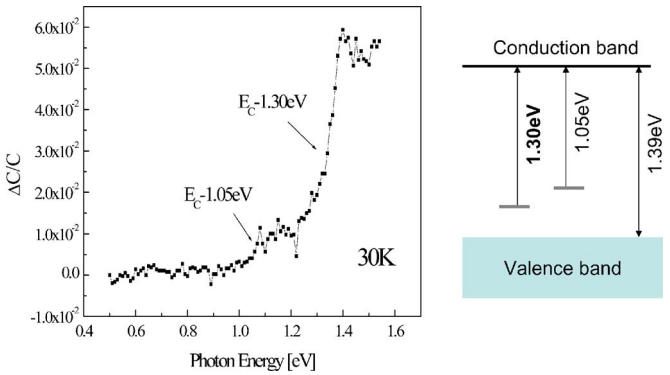

FIG. 3. (Color online) 30 K-photocapacitance spectra of LPE-grown InP layers with a dislocation-free ELO layer and the corresponding optical transitions shown by simple flat-band diagrams.

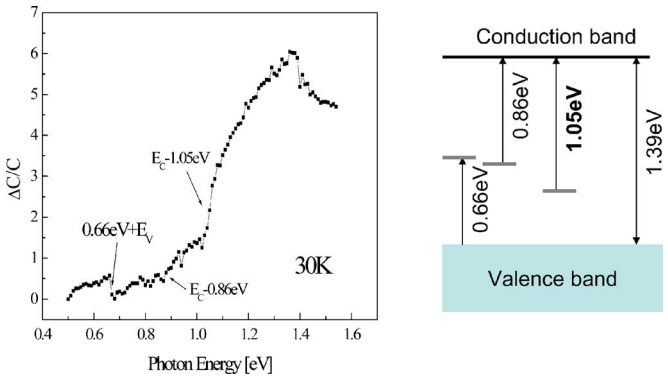

FIG. 4. (Color online) 30 K-photocapacitance spectra of LPE-grown InP layers with a dislocated small-area SB junction at the coalescent region formed by the two dislocation-free ELO layers and the corresponding optical transitions as a simple flat-band diagram.

tem will be referred to elsewhere.[23] The detailed emission and capture characteristics were investigated by the excitation photocapacitance measurements, and this is also referred to elsewhere.[24] Excitation photocapacitance measurements were carried out at 30 K. Sample diodes were forward-biased in the dark to neutralize every deep level. Then the primary excitation monochromatic light ($h\nu_1$) is illuminated into the depletion layer and then the ion density photocapacitance spectrum was measured from the long wavelength ($h\nu_2$). When the ion density shows its saturating value, the charge state of the level changes from its neutral state to the ionized state. Thus, the successive long wavelength light ($h\nu_2$) detected the optical transition from valence band (VB) to the ionized state.

The arrival at saturating ion density by the primary excitation light ($h\nu_1$) illumination was automatically detected by our photocapacitance measurement system through the *in situ* derivative calculations of the photocapacitance signal. And, the steady state ion density by the $h\nu_2$ illumination is also obtained automatically when the photocapacitance signal is well stabilized. The energy interval of primary excitation light ($h\nu_1$) is 20 meV, and that for ion density photocapacitance spectra measurements ($h\nu_2$) is 10 meV. Resolution of the excitation light source fed from the monochromator is well below 1 meV in this spectral region. In the photocapacitance spectra, the means of identification of the levels is to find the steepest increase in the capacitance at a given photon energy.

III. RESULTS AND DISCUSSIONS

Figures 1 and 2 show the sample configurations of the Au-wire bonded ELO layers and corresponding schematic drawings of the cross-sectional structures. In Fig. 1, a point-contact SB junction was formed on the dislocation-free ELO layer, where Huber etching does not reveal any dislocation etch pits. Figure 2 shows a point-contact SB junction formed on a specific dislocated region, where the two dislocation-free ELO layers coalescence.

Figures 3 and 4 show the 30 K-photocapacitance spectra of LPE-grown InP layers with a dislocation-free ELO layer and a dislocated small-area SB junction at the coalescent region of two L-shaped open seeds, respectively. In the insets of the figures, the corresponding optical transitions are shown as simple flat-band diagrams.

It is shown that the only dominant deep level is located at almost E_c 1.30 eV in the dislocation-free ELO layer with a deep-level density of $\Delta C/C(\propto N_T)=5\times10^{-2}$. On the other hand, it is also clearly shown that additional dominant deep levels can be detected at E_c 0.86 eV and 1.05 eV when the deep-level densities are $\Delta C/C(\propto N_T)=1$ *and* 4, 5, respectively. In addition, the neutralized gap state is also detected at 0.66 eV+E_v when $\Delta C/C(\propto N_T)=0.5$. Table I summarizes the deep levels detected in the dislocated and dislocation-free small-area SB junctions by the present photocapacitance measurements. When the photocapacitance results from the dislocation-free SB junction were compared with those of dislocated SB junctions, it is considered that the dislocations induced the electronic deep states that occur at E_c 0.86 eV and 1.05 eV.

In order to clarify the detailed optical transition mechanisms of the dislocation-induced deep levels, 30 K-excitation photocapacitance measurements were applied to a dislocated small-area SB junction that was formed on the coalescent

TABLE I. Deep levels in dislocation-free and dislocated ELO InP.

	Dislocation-free ELO	$\Delta C/C$ $\propto N_T$	Dislocated ELO Coalescent L-shaped open seeds	$\Delta C/C$ $\propto N_T$
Ionization	E_c 1.30 eV	5×10^{-2}	E_c 0.86 eV	~1
	E_c 1.05 eV	1×10^{-2}	E_c 1.05 eV	~4.5
Neutralization			0.66 eV+E_v	0.5

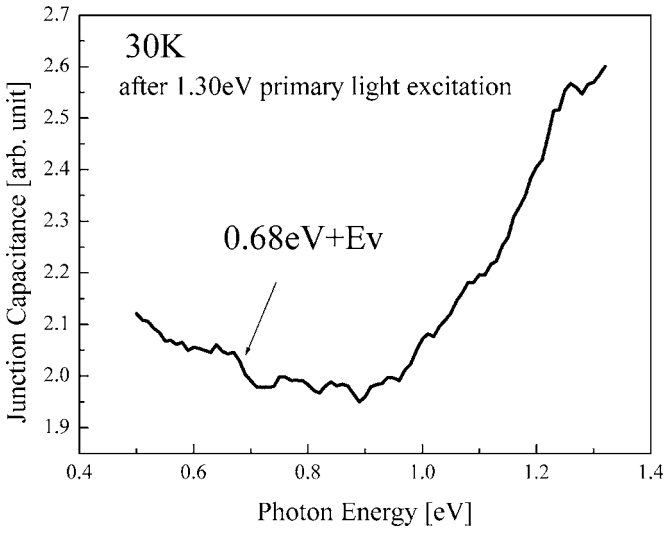

FIG. 5. Typical excitation photocapacitance spectrum when 1.30 eV primary excitation light was irradiated, after which monochromatic light is irradiated from the long wavelength in order to detect the neutralization at 0.68 eV above the valence band.

region formed by two L-shaped dislocation-free ELO layers. The primary excitation monochromatic light was irradiated from 0.5 to 1.40 eV with an interval of 20 meV, and then the change in junction capacitance was measured in the spectral range between 0.5–1.3 eV with an interval of 10 meV. Figure 5 shows a typical excitation photocapacitance spectrum when 1.30 eV primary excitation light was irradiated. It is shown that the neutralization of an ionized deep level, which was ionized by the primary excitation light, was detected at 0.68 eV, which means that the neutralized level is located at 0.68 eV+E_v. This 0.68 eV+E_v neutralized level was detected just after the 1.30 eV primary excitation light was irradiated. From this result, it is considered that the defect configuration coordinate diagram is as shown in Fig. 6, and the Frank-Condon shift value (d_{FC}) of the dislocation-related

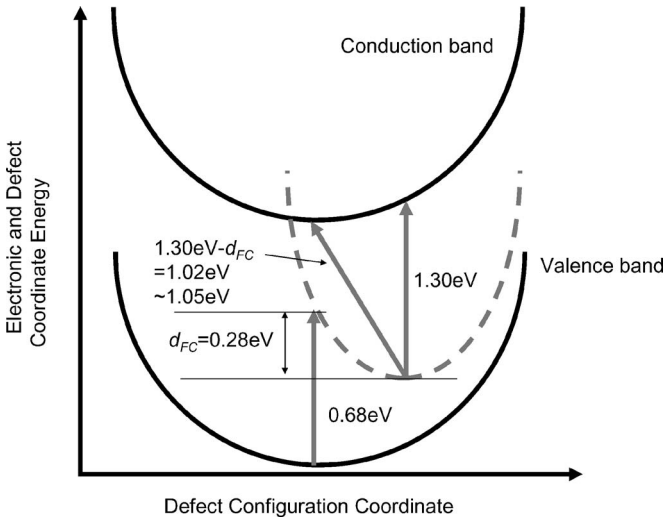

FIG. 6. Configuration coordinate diagram for the dislocation-induced deep level deduced from the excitation photocapacitance results.

deep level was determined to be 0.28 eV. This result coincides well with the photocapacitance spectrum shown in Fig. 4, because if d_{FC}=0.28 eV, it is expected that the indirect excitation photon energy for the 1.30 eV level will be 1.02 eV, which is very similar to the ionization energy of E_c 1.05 eV that appeared in Fig. 4.

As shown in the above results, it is noticed that the dislocation-induced deep level has exhibited a large Frank-Condon shift, which reflects the strained atomic configuration around the defect level. One of the well-known deep levels with a large value of d_{FC} is the so-called "DX center" in AlGaAs.[25] The DX center in AlGaAs shows a large d_{FC} of about 1.0 eV. It has been reported that the defect structure of the DX center is the donor-Ga vacancy complex, with a large lattice strain around the defect. Actually, precise x-ray diffraction measurements revealed a large lattice strain corresponding to the ionization of the DX center by monochromatic light irradiation.[26] The DX center has also been reported in other compound semiconductor systems such as GaAlSb.[27]

The EL2 level in GaAs is also a well-investigated deep level with a large d_{FC} of 0.12 eV. This d_{FC} value is consistent with the reported results from Yu's early PL work[28] and our recent excitation photocapacitance results.[24] Whereas the EL2 defect is closely related with an excess arsenic composition in GaAs, the detailed configuration of the defect is still under discussion. Since the early simple model of an isolated arsenic antisite defect (As_{Ga}) was proposed, numerous defect models that include the As_{Ga} defect complex[29] have been presented both experimentally and theoretically. The strain effect around the EL2 defect is also reported on the basis of light-induced changes in the defect structure.[30] Indeed, it has been reported that the full width at half-maximum (FWHM) values of precise x-ray rocking curves and the lattice constant were changed due to ionization and photoquenching at low temperature.[31] However, many reports have been carried out covering low-temperature-grown (LT) GaAs, in which the As_{Ga} concentration is extremely high; in the order of 10^{20} cm^{-3}. The EL2 concentration in semi-insulating (SI) GaAs is about 2×10^{16} cm^{-3}, and thus it is noticed that the defect structure in LT-GaAs and SI GaAs will not be exactly the same. Other examples of defect deep-levels with large d_{FC} are the 1 MeV electron-irradiation induced defects i *p*-InGaP (Ref. 32) neutron-irradiated GaN (Ref. 33) and the stoichiometry-dependent deep levels in GaAs,[34] respectively.

These deep levels with large d_{FC} values are accompanied by a large lattice strain around the defects, and the defect structure is not a simple substitution of defects or impurities, but a complex aggregation of a few defects. Indeed, a very small d_{FC} (in the order of 10 meV) was reported for the almost-complete substitution of impurities in the matrix lattice.[35] Thus, it is considered that the present dislocation-related deep level with a large d_{FC} is due to the large lattice strain at the dislocation core.

When dislocation-related deep levels are discussed, the effects of impurities are crucial. As is well known for the Cottrell atmosphere,[12] impurities in the solid have a tendency to aggregate around dislocations to compensate the lattice strain around the dislocations. The technique known as "intrinsic gettering technology[36]" is based on this phenomenon,

and is designed to improve device performance by the gettering of heavy metal impurities from the electron channels in silicon metal-oxide-semiconductor (MOS) devices. Indeed, the effects of the aggregation of impurities on dislocation-related deep levels have already been reported.[37]

In terms of the effects of impurities on the present dislocation-related deep levels, it is noticed that conductivity type is *n*-type and that the residual impurity concentration is about 3×10^{16} cm^{-3} with a donor activation energy of about 5 meV. The chemical species that form the residual impurities have not been clarified. The obtained donor activation energy is very similar to that of the Rydberg binding energy (E_{Ryb}=7.31 meV), which is calculated from the effective mass approximation (m_n=0.073m_0, ε_s=12.56ε_0). When the transition metals or heavy metals such as Cu, Mn, Fe, and Cr are incorporated into InP, these impurities usually act as a deep acceptor, and thus the conductivity type will show as *p*-type. In addition, the activation energy of these impurities is large compared with those of shallow levels. SIMS was applied to the present ELO layers. The positive and negative SIMS analyses also fail to reveal any trace of heavy impurity contamination, such as Fe and Cu. From these results, the present specimens are free from serious contamination from impurities.

IV. CONCLUSIONS

In summary, the 30 K-photocapacitance measurements revealed the presence of dislocation-related deep levels in ELO layers of InP prepared by high purity liquid phase epitaxy. When the photocapacitance spectra were compared with those of dislocation-free ELO layers, which were also grown epitaxially at the same time and on the same substrate, it is considered that the dislocations form deep donor levels at 0.86 and 1.05 eV below the conduction band. The excitation photocapacitance results show the detailed emission and capture optical transitions, and it is shown that the dislocation-related deep level is followed by a large Frank-Condon shift (d_{FC}) of 0.28 eV, and thus large lattice relaxation around the defects should be considered.

[1] R. Labusch and W. Schröter, in *Dislocations in Solids*, edited by F. R. N. Nabarro (North-Holland, Amsterdam, 1980), Vol. 5, p. 128. H. Alexander, in *Dislocations in Solids* (Ref. 1), Vol. 7, p. 118; H. Alexander and H. Teichler, in *Materials Science and Technology*, edited by R. W. Cahn, P. Haasen, and E. J. Kramer (VCH Weinheim, Cambridge, 1993), Vol. 4, p. 249.

[2] A. Cavallini, B. Fraboni, S. Pizzini, S. Binetti, L. Lazzarini, and G. Salviati, J. Lumin. **80**, 343–346 (1999).

[3] V. Kveder, M. Badylevich, W. Schroter, M. Seibt, E. Steinman, and A. Izotov, Phys. Status Solidi A **202**, 901 (2005).

[4] Niklas Lehto, Phys. Rev. B **55**, 15601 (1997); A. Castaldini, D. Cavalcoli, A. Cavallini, and S. Pizzini, Phys. Rev. Lett. **95**, 076401 (2005).

[5] C. Kisielowski and E. R. Weber, Phys. Rev. B **44**, 1600 (1991).

[6] A. Castaldini, D. Cavalcoli, A. Cavallini, and S. Pizzini, Phys. Rev. Lett. **95**, 076401 (2005).

[7] M. Seibt, V. Kveder, W. Schroter, and O. Voß, Phys. Status Solidi A **202**, 911 (2005).

[8] S. Binetti, S. Pizzini, E. Leoni, and R. Somaschini, A. Castaldini, and A. Cavallini, J. Appl. Phys. **92**, 2437 (2002).

[9] C. Kisielowski, J. Palm, B. Bollig, and H. Alexander, Phys. Rev. B **44**, 1588 (1991).

[10] C. R. Moon, In Kim, Jeong Seok Lee, Byung-Doo Choe, S. D. Kwon, and H. Lim, Appl. Phys. Lett. **70**, 3284 (1997); D. Pal, E. Gombia, R. Mosca, A. Bosacchi, and S. Franchi, J. Appl. Phys. **84**, 2965 (1998).

[11] Klaus Knobloch, Martin Kittler, and Winfried Seifert, J. Appl. Phys. **93**, 1069 (2003); O. F. Vyvenko, M. Kittler, W. Seifer, and M. V. Trushin, Phys. Status Solidi C **2**, 1852 (2005).

[12] A. H. Cottrell, *Report on the Strength of Solids* (Physical Society, London, 1948), p. 30; Proc. Phys. Soc. London **62**, 49 (1949); in *Progress in Metal Physics* (Interscience, New York, 1949), Chap. 2; *Theory of the Yield Point of Iron* (British Iron and Steel Res. Assoc, 1948).

[13] A. T. Blumenau, R. Jones, S. Öberg, P. R. Briddon, and T. Frauenheim, Phys. Rev. Lett. **87**, 187404 (2001).

[14] T. Y. Tan, E. E. Gardner, and W. K. Tice, Appl. Phys. Lett. **30**, 175 (1977).

[15] J. Wiebe, L. Sacharow, A. Wachowiak, G. Bihlmayer, S. Heinze, S. Blügel, M. Morgenstern, and R. Wiesendanger, Phys. Rev. B **70**, 035404 (2004).

[16] J. A. Friedrich, M. Kastelic, G. W. Neudeck, C. G. Takoudis, J. Appl. Phys. **65**, 1713 (1989).

[17] Shuji Nakamura, Masayuki Senoh, Shin-ichi Nagahama, Naruhito Iwasa, Takao Yamada, Toshio Matsushita, Hiroyuki Kiyoku, Yasunobu Sugimoto, Tokuya Kozaki, Hitoshi Umemoto, Masahiko Sano, and Kazuyuki Chocho, Jpn. J. Appl. Phys., Part 2 **37**, L309 (1998).

[18] Akira Sakai, Haruo Sunakawa, and Akira Usui, Appl. Phys. Lett. **73**, 481 (1998).

[19] V. Wagner, O. Parillaud, H. J. Bühlmann, M. Ilegems, S. Gradecak, P. Stadelmann, T. Riemann, and J. Christen, J. Appl. Phys. **92**, 1307 (2002).

[20] Toshio Kochiya, Yutaka Oyama, Toshihiro Kimura, Ken Suto, and Jun-ichi Nishizawa, J. Cryst. Growth **281**, 263 (2005).

[21] J. Nishizawa, Y. Okuno, and H. Tadano, J. Cryst. Growth **31**, 15 (1975); J. Nishizawa and Y. Oyama, Mater. Sci. Eng., R. **12**, 273 (1994).

[22] A. Huber and N. T. Linh, J. Cryst. Growth **29**, 80 (1975).

[23] Jun-ichi Nishizawa, Yutaka Oyama, and Kazushi Dezaki, Phys. Rev. Lett. **65**, 2555 (1990).

[24] Yutaka Oyama and Jun-ichi Nishizawa, J. Appl. Phys. **97**, 033705 (2005).

[25] D. V. Lang and R. A. Logan, Phys. Rev. Lett. **39**, 635 (1977); J. Nishizawa and K. Suto, J. Appl. Phys. **48**, 3484 (1977).

[26] G. S. Cargill, III, A. Segmüller, T. F. Kuech, and T. N. Theis, Phys. Rev. B **46**, 10078 (1992); M. Leszczynski, *ibid.* **48**, 17046 (1993); Armin Segmüller, J. Vac. Sci. Technol. A **9**, 2477 (1991).

[27] A. Baraldi, C. Ghezzi, R. Magnanini, A. Parisini, L. Tarricone,

and S. Zerbini, J. Appl. Phys. **83**, 491 (1998).
[28] P. W. Yu, Phys. Rev. B **42**, 11889 (1990).
[29] A. Fukuyama, T. Ikari, Y. Akashi, and M. Suemitsu, Phys. Rev. B **67**, 113202 (2003).
[30] V. Pandian and V. Kumar, J. Appl. Phys. **70**, 5114 (1991).
[31] M. Leszczynski, Phys. Rev. B **48**, 17046 (1993); H. Fujioka, J. Krueger, A. Prasad, X. Liu, and E. R. Weber, J. Appl. Phys. **78**, 1470 (1995).
[32] M. Adachi, A. Khan, K. Ando, N. J. Ekins-Daukes, H. S. Lee, and M. Yamaguchi, Phys. Rev. B **72**, 155320 (2005).
[33] S. Li, J. D. Zhang, C. D. Beling, K. Wang, R. X. Wang, M. Gong, and C. K. Sarkar, J. Appl. Phys. **98**, 093517 (2005).
[34] Jun-ichi Nishizawa, Yutaka Oyama, and Kazushi Dezaki, J. Appl. Phys. **67**, 1884 (1990); **70**, 833 (1991).
[35] H. Pettersson, H. G. Grimmeiss, K. Schmalz, A. Knecht, and R. Passler, J. Appl. Phys. **77**, 2495 (1995).
[36] T. Y. Tan, E. E. Gardner, and W. K. Tice, Appl. Phys. Lett. **30**, 175 (1977).
[37] V. Kveder, M. Kittler, and W. Schröter, Phys. Rev. B **63**, 115208 (2001); O. F. Vyvenko, M. Kittler, and W. Seifert, J. Appl. Phys. **96**, 6425 (2004); M. Seibt, V. Kveder, W. Schröter, and O. Voß, Phys. Status Solidi A **202**, 911 (2005).